JOURNAL OF MAGNETIC RESONANCE **131,** 126–130 (1998)
ARTICLE NO. MN971352

Temperature Imaging by ^{1}H NMR and Suppression of Convection in NMR Probes

N. Hedin and I. Furó[1]

Division of Physical Chemistry, Department of Chemistry, Royal Institute of Technology, SE-10044 Stockholm, Sweden

Received September 19, 1997

A simple arrangement for suppressing convection in NMR probes is tested experimentally. Diffusion experiments are used to determine the onset of convection and ^{1}H temperature imaging helps to rationalize the somewhat surprising results. A convenient new ^{1}H NMR thermometer, CH_2Br_2 dissolved in a nematic thermotropic liquid crystal, is presented. © 1998 Academic Press

Key Words: **convection; diffusion; PGSE; temperature imaging.**

INTRODUCTION

Many NMR experiments, in particular diffusion studies that detect the motion of molecules on the micrometer length scale, require an excellent mechanical stability of the experimental setup. While this is relatively straightforward to provide for the various mechanical parts of the probe, liquid samples often present a problem; a fluid enclosed in a cell located in a gravity field and heated from below may experience natural convection heat transfer. The onset of (Bénard) convection (*1, 2*) is marked by the so-called Rayleigh number Ra, which depends on the material constants of the fluid and the longitudinal temperature gradient, exceeding a critical value Ra_c, which is defined by the geometry of the enclosure and the boundary conditions on it. The various designs, invented to avoid convection, usually modify the last three of these four variables. In this paper we present an investigation of the simple counterconvective measure that we found useful in our temperature-dependent PGSE diffusion studies that are aimed at accurate diffusion coefficients measured in various surfactant solutions.

CONVECTION: THEORY AND THE DESIGN OF NMR PROBES

First, we briefly recall some essential points regarding fluid convection. For a Newtonian fluid the convection problem can be readily analyzed (*1, 2*) in the two limiting cases of cylindrical symmetry, the infinitely wide layer and the infinitely long tube. The Rayleigh number Ra for these two limiting cases can be expressed as

$$\mathrm{Ra}_{\mathrm{layer}} = \frac{g\alpha}{\kappa\nu} L^4 \dot{T} \qquad [1]$$

for the layer case and

$$\mathrm{Ra}_{\mathrm{tube}} = \frac{g\alpha}{\kappa\nu} r^4 \dot{T} \qquad [2]$$

for the tube case, where L is the fluid height and r is the tube radius (corresponding to the inner radius of the NMR tube); g is the acceleration due to gravity; $\dot{T}$ is the vertical temperature gradient; and α, ν, and κ are the coefficients of thermal expansion, kinematic viscosity, and thermal diffusivity of the fluid, respectively. In these ideal geometries the onset of the convection appears when (*3*)

$$\begin{aligned} \mathrm{Ra}_{\mathrm{layer}} > 720 \quad &\text{(for rigid insulating walls)} \\ 1708 \quad &\text{(for rigid conducting walls)} \end{aligned} \qquad [3]$$

for the layer case and

$$\begin{aligned} \mathrm{Ra}_{\mathrm{tube}} > 67.4 \quad &\text{(for rigid insulating walls)} \\ 215.8 \quad &\text{(for rigid conducting walls)} \end{aligned} \qquad [4]$$

for the tube case; the right-hand figures are the theoretical Ra_c's. For finite cylindrical enclosures numerical analysis (*4, 5*) yields that Ra_c may change by one order of magnitude between the axial ratios of 2 and 1. (The axial ratio here is defined as $\rho = L/r$, that is, the inverse of the axial ratio defined in the frequently cited papers of Charlson and Sani (*4, 5*).) Typical NMR samples have axial ratios of 3 (for 10-mm tubes) to 10 or higher (for 5-mm tubes); in the $\rho \geq 3$ region the theoretical value of Ra_c is essentially constant (*4, 5*) if Ra is calculated (*6*) as defined by Eq. [2]. Similarly, Ra_c is essentially constant for cylindrical fluid layers of axial ratios of 0.3 and below if Ra is calculated as defined by Eq.

[1] To whom correspondence should be addressed. Fax: +46 8 7908207. E-mail: ifuro@physchem.kth.se.

1090-7807/98 $25.00

[1]. (It is impractical to present the stability condition for long objects like NMR samples in terms of Eq. [1]. The resulting numbers are high to astronomical and difficult to perceive and use.) Hence, for typical NMR samples the theory yields that the onset of convection should happen at temperature gradients

$$\dot{T} > \frac{\kappa\nu}{g\alpha}\,\frac{\mathrm{Ra_c}}{r^4}, \qquad [5]$$

where $\mathrm{Ra_c}$ is close to the figures given in Eq. [4].

However, these ideal geometries may have little bearing on the experimental situation encountered in a particular NMR probe (see our experiences below). There, the wall properties and other boundary conditions, most importantly the temperature distribution, are poorly characterized and the sample geometry deviates from the ideal tube case. Qualitatively, however, the r^4 dependence makes that 10-mm tubes are far more prone to convection. The onset of convection in a particular NMR setup should be determined, though, via experiments.

There are large differences in NMR probe design between different vendors. Generally, counterflow arrangements for the regulation air found, for example, in the high-resolution probes of Bruker provide small gradients. A less suitable construction is to let the regulation air flow into the probe space directly from below (measuring below room temperature by cooling from below is convection-free). Perhaps because of the lack of space such a lamentable arrangement is rather usual in diffusion probes such as the one used in this study.

There are several possible solutions for reducing convection. First, the probe can be rebuilt either so that counterflow of the regulation air reduces the temperature gradient or so that for measuring at higher than room temperatures the sample is heated from above (*7*). Second, the sample can be enclosed in a circulating fluid bath that strongly reduces the temperature gradient (*8, 9*). These options might be too complex, expensive, or time-consuming. Third, sample rotation (as used for reducing convection artifacts in inversion recovery experiments (*10*)) suppresses convection (*11*) but this is, of course, unsuitable for diffusion experiments. Fourth, one may increase the flow rate of the air (*12*); this particular remedy proved to be less helpful for us. Fifth, one could eventually use 3-mm tubes (*7*). As another possibility, pulse sequences are available for diffusion measurements that cancel effects from coherent motions like convection (*13–15*). However, those techniques might be difficult to adapt on simple gradient power supplies and, moreover, acceleration effects, which as well exist in the convecting sample, are not canceled by them. Therefore, we chose the simple arrangement presented below.

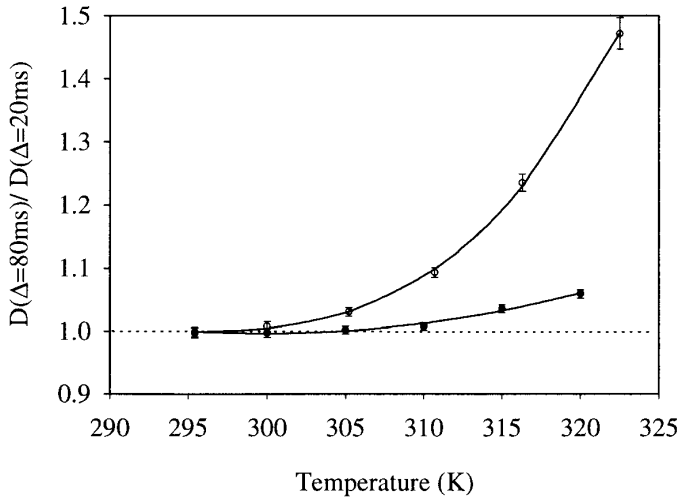

FIG. 1. The temperature variation of the ratio of the diffusion coefficients measured by PGSE experiments (*16*) with different diffusion times Δ. The error bars show the propagated random error obtained from the fits of the individual diffusion experiments. The filled and open symbols are the results with and without Krytox oil surrounding the sample, respectively. Apparent Δ-dependent diffusion coefficients that indicate convection show up in the figure as a deviation from the dashed line at 1; the solid lines are (cubic) guides to the eye.

DIFFUSION EXPERIMENTS

The PGSE probehead attached to our Bruker AMX-300 spectrometer was purchased from Cryomagnet Systems (Indianapolis, IN). The temperature regulation uses pressurized air (usually about 90 L/min) led directly into the sample space from below; at moderately higher-than-room temperatures PGSE experiments (*16*) often provided gradient-dependent lineshape distortions in experiments on 10-mm tubes, indicating the presence of convective heat transfer. As expected from Eq. [5] experiments on 5-mm tubes at temperatures 15–25 K over room temperature provided no phase error; this, however, is not a sufficiently rigorous test for the absence of convection. Instead, the onset of convection can be more sensitively detected by comparing diffusion coefficients measured at different diffusion times Δ. (Direct velocity imaging (*17*) might be another option.) Since coherent (such as convection) and incoherent (such as diffusion) motions have different time propagators convection shows up as a Δ-dependent (apparent) diffusion coefficient (*15*). Conversely, the observed absence of Δ dependence indicates that diffusion measurements performed with similar experimental parameters are free from convection effects.

Our results obtained for water in a 5-mm NMR tube placed concentrically in a 10-mm NMR tube (with a distance of 5 mm between the tube bottoms) are shown in Fig. 1; the behavior in a free-standing 5-mm tube is rather similar. Since we intended to perform experiments around 310 K, where Fig. 1 indicates convection, this arrangement was un-

suitable for us. Plausibly (and, as shown below, somewhat incorrectly), one expects a reduction of the temperature gradient within the sample by filling a liquid that has a higher heat capacity than the air in between the 5-mm and 10-mm tubes. We chose the perfluorinated oil Krytox 143 AZ (DuPont, M_W 1850) for filling up the intertube space until 0.5 cm over the sample surface. This fluid provides a small ^{1}H background signal with a large chemical shift and has a high heat capacity. The diffusion results in Fig. 1 show that the onset of the convection is indeed delayed by this arrangement. The absence of convection effects to better than 1% accuracy at 310 K was sufficient for our planned experiments.

^{1}H NMR TEMPERATURE SENSOR AND TEMPERATURE IMAGING

To make sure that the observed suppression of convection is not due to an increased difference between the set and the actual sample temperatures and to visualize the (assumed) reduction of the temperature gradient in the sample, we chose to monitor and control the sample temperature directly by NMR means. Although sensitive temperature standards are readily available for many heteronuclei such as ^{59}Co (*7, 18*), sensitive (with <0.1 K resolution) ^{1}H temperature standards (thus suitable for our ^{1}H PGSE probe) are rare. (The frequently chosen methanol and ethylene glycol systems (*19–21*) do not provide sufficient temperature resolution.)

Dibromomethane (CH_2Br_2) dissolved at 5 wt% in N4 liquid crystal (Merck; nematic between 293 and 348 K) and flame sealed proved to be a suitable *in situ* ^{1}H temperature sensor. Just like in the more familiar case of benzene dissolved in a thermotropic liquid crystal (*22*) the residual static dipole–dipole coupling caused by the anisotropic orientational order provides a static splitting of the ^{1}H spectrum. Dibromomethane has several advantages over benzene. First, there are only 2 narrow ^{1}H lines in contrast to the >60 lines for benzene (*22*) which leads to a better signal-to-noise ratio. Second, the two coupled protons form an $I = 1$ spin system of a well-known spin dynamics where, for example, the homogeneous linewidth (which is necessary to establish the temperature resolution) can easily be obtained by the quadrupolar echo method (*23*). At around 305 K the temperature dependence of the splitting is 40 Hz/K ($\sim$60 Hz/K at 315 K) and the homogeneous linewidth is about 1 Hz; ideally, this provides a temperature resolution far better than 0.1 K. Third, the boiling point of dibromomethane (98°C) is higher than that of benzene (80°C), providing better sample stability at high temperatures.

The sample arrangements with and without Krytox as presented above have been tested by replacing the water sample with the liquid crystal with dissolved CH_2Br_2. Since the viscosity of the liquid crystal is 100 times that of water there was no convection in the liquid crystal sample. The magnetic field had been first shimmed at room temperature and without temperature regulation; under such conditions the temperature gradient is very small which provides narrow lines that are predominantly broadened by magnetic field inhomogeneity. After the sample was warmed up to the temperature to be investigated the shims were slightly adjusted to provide the most narrow and antisymmetric (to each other) ^{1}H lines. Quadrupolar echo experiments with and without refocusing the magnetic field inhomogeneity (*24*) showed that the remaining broadening of the ^{1}H lines was dominated by an inhomogeneous distribution of the dipole splitting.

The *in situ* temperature test has shown that the actual temperatures in the two sample arrangements were close to each other. Using the measured splittings, the diffusion data in Fig. 1 are already presented on a common temperature scale calibrated by the measured splittings; notice the slight but increasing shift between the experimental set temperatures. The initial temperature studies provided us with two surprises. First, the ^{1}H linewidths and, thus, the temperature differences over the sample volumes were almost the same with and without Krytox; in other words, the method worked but we did not know why. Second, the onset of convection happened at very small temperature gradients, much below the theoretical value which is about 7.0–2.8 K/cm (for conducting wall) or about 2.2–0.85 K/cm (for insulating wall) for a 5-mm (4.3-mm-i.d.) tube in the region of 293–313 K as provided by Eqs. [4] and [5] and by the literature values of the (temperature-dependent) material constants for water (*2*). (We note that the theoretical onset gradients calculated in Ref. (*10*) are wrong by a factor of 100.) In the arrangement with Krytox, the temperature gradient (defined as the full temperature difference over the sample volume deducted from the ^{1}H linewidth divided by the 4-cm length of the sample) at 315 K where Fig. 1 indicates convection is about 0.2 K/cm. The temperature gradient at 305 K in the other arrangement without Krytox is even smaller, about 0.03 K/cm. Others have observed similar early onset of convection (*7*).

To see what has caused then the reduction of convection and what might be the cause of the early onset of convection as witnessed by Fig. 1 a simple 1D imaging experiment was performed. The experiment uses the simple spin-echo pulse sequence

$$(\pi/2)-t_1/2-(\pi)-t_1/2-t_2\text{:acq} \qquad [6]$$

with Exorcycle (*25*) for the RF phases that is performed in the presence of a small ($\sim$8 G/m) constant z gradient. During t_1 the magnetic field inhomogeneity is refocused while the dipolar broadening evolves undisturbed; the signal detected during t_2 is dominantly broadened by the applied small z gradient. Hence, the resulting 2D spectrum provides the distribution of the temperature along the z direction. The results obtained at 320 K are presented in Fig. 2.

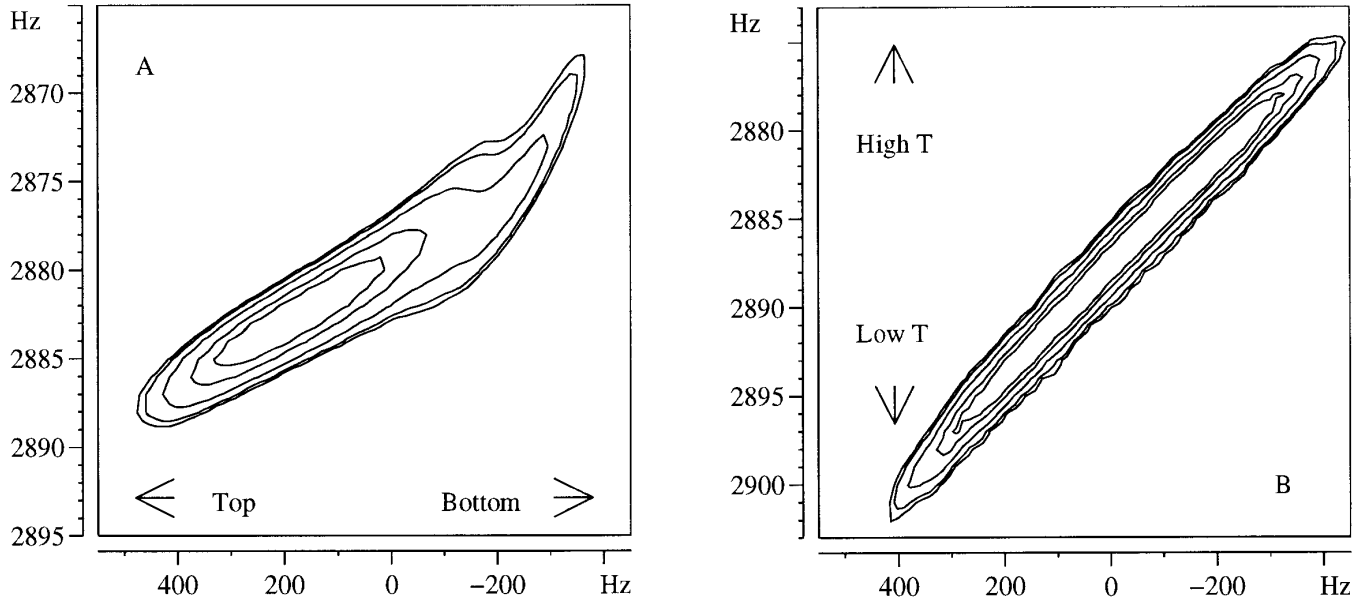

FIG. 2. 2D contour plots of the temperature imaging experiment using the spin-echo pulse sequence in Eq. [6] performed at 320 K without (A) and with (B) Krytox oil bath. The horizontal frequency scale corresponds to the position along the *z* axis with a resolution of about 200 Hz/cm. The vertical frequency axis provides the temperature variation by a resolution of 67 Hz/K (obtained from the variation of the dipolar line splitting at around 320 K).

Clearly, without Krytox the bottom of the sample has a much larger temperature gradient than the top which may lead to an early onset of a local convection cell. Moreover, in this setup there seems to exist a temperature gradient perpendicular to the coil axis (observed as larger width of vertical cross sections) as well, which also becomes stronger toward the bottom of the sample. In any case, it is as yet unclear to us from the convection literature (*2, 3, 26*) what would be the effect of a highly nonlinear temperature distribution on the onset of convection. Filling the inner-tube space with Krytox makes the temperature gradient more constant all along the sample which raises the full temperature difference for convection onset fivefold. Still, however, the experimental onset gradient is by at least a factor of 4 lower than that suggested by the theory. As yet, we have found no convincing explanation for this discrepancy; convection experiments with better control of the boundary conditions yielded results that conform to the theory (*27–30*).

CONCLUSIONS

Convection in the sample should be suppressed in NMR experiments by a proper design of the probe. As demonstrated above, a simple way of suppressing convection in a typical probe design is to immerse the sample into a small static bath of Krytox oil. This arrangement allowed us to measure accurately diffusion coefficients at temperatures where diffusion measurements without the oil bath were corrupted by convection effects. As shown by our temperature imaging experiments the primary effect of the oil surrounding the NMR sample is to even out the temperature gradient along the sample axis and possibly decrease it perpendicular to the axis; the temperature gradient at the onset of the convection (as detected by NMR diffusion measurements) is, however, still significantly lower than the value predicted by theory. Some of these results could be kept in mind when planning high-temperature experiments with NMR methods that are in any way sensitive to sample motion.

ACKNOWLEDGMENTS

This work has been supported by the Swedish Natural Science Research Council (NFR). N.H. thanks the Ernst Johnsson Foundation for a scholarship. Helpful comments from Peter Stilbs are much appreciated.

REFERENCES

1. L. D. Landau and E. M. Lifshitz, ''Fluid Mechanics,'' Pergamon, Oxford (1987).
2. A. Bejan, ''Convection Heat Transfer,'' Wiley, New York (1995).
3. C. Normand and Y. Pomeau, *Rev. Mod. Phys.* **49,** 581 (1977).
4. G. S. Charlson and R. L. Sani, *Int. J. Heat Mass Transfer* **13,** 1479 (1970).
5. G. S. Charlson and R. L. Sani, *Int. J. Heat Mass Transfer* **14,** 2157 (1971).
6. C. Guthman, B. Perrin, and H. Thomé, *J. Phys. Fr.* **50,** 2951 (1989).
7. W. J. Goux, L. A. Verkruyse, and S. J. Salter, *J. Magn. Reson.* **88,** 609 (1990).
8. D. J. Greensdale and M. Judd, *J. Phys. E* **6,** 101 (1973).

9. N. Boden, S. A. Corne, P. Halford-Maw, D. Fogarty, and K. W. Jolley, *J. Magn. Reson.* **98,** 92 (1992).

10. J. Lounila, K. Oikarinen, P. Ingman, and J. Jokisaari, *J. Magn. Reson. A* **118,** 50 (1996).

11. H. T. Rossby, *J. Fluid Mech.* **36,** 309 (1969).

12. A. Allerhand, R. Addleman, and D. Osman, *J. Am. Chem. Soc.* **107,** 5809 (1985).

13. Y. Xia and P. T. Callaghan, *Macromolecules* **24,** 4777 (1991).

14. A. Jerschow and N. Müller, *J. Magn. Reson.* **125,** 372 (1997).

15. P. T. Callaghan, ''Principles of Nuclear Magnetic Resonance Microscopy,'' Clarendon, Oxford (1991).

16. P. Stilbs, *Prog. NMR Spectrosc.* **19,** 1 (1987).

17. B. Manz, J. D. Seymour, and P. T. Callaghan, *J. Magn. Reson.* **125,** 153 (1997).

18. G. C. Levy, J. T. Bailey, and D. A. Wright, *J. Magn. Reson.* **37,** 353 (1980).

19. A. L. v. Geet, *Anal. Chem.* **42,** 679 (1970).

20. D. S. Raiford, C. L. Fisk, and E. D. Becker, *Anal. Chem.* **51,** 2050 (1979).

21. C. Amman, P. Meier, and A. E. Merbach, *J. Magn. Reson.* **46,** 319 (1982).

22. R. D. Farrant and J. C. Lindon, *Magn. Reson. Chem.* **32,** 231 (1994).

23. J. H. Davis, K. R. Jeffrey, M. Bloom, M. I. Valic, and T. P. Higgs, *Chem. Phys. Lett.* **42,** 390 (1976).

24. I. Furó and B. Halle, *J. Magn. Reson.* **98,** 388 (1992).

25. G. Bodenhausen, R. Freeman, and D. L. Turner, *J. Magn. Reson.* **27,** 511 (1977).

26. F. H. Busse, *Rep. Prog. Phys.* **41,** 1929 (1978).

27. I. Catton and D. K. Edwards, *J. Heat Transfer* **87,** 295 (1967).

28. J. D. Verhoeven, *Phys. Fluids* **12,** 1733 (1969).

29. I. Catton and D. K. Edwards, *AIChE J.* **16,** 594 (1970).

30. K. Stork and U. Müller, *J. Fluid Mech.* **71,** 231 (1975).